Molecular Biology of the Cell
Vol. 19, 3272–3282, August 2008

MicroRNA-21 Targets Sprouty2 and Promotes Cellular Outgrowths

Danish Sayed,* Shweta Rane,* Jacqueline Lypowy,*† Minzhen He,* Ieng-Yi Chen,* Himanshu Vashistha,‡ Lin Yan,* Ashwani Malhotra,‡ Dorothy Vatner,* and Maha Abdellatif*

*Cardiovascular Research Institute, Department of Cell Biology and Molecular Medicine, and Department of Medicine, and ‡Division of Nephrology, University of Medicine and Dentistry of New Jersey, Newark, NJ 07103

Submitted February 15, 2008; Revised May 19, 2008; Accepted May 21, 2008
Monitoring Editor: Jonathan Chernoff

The posttranscriptional regulator, microRNA-21 (miR-21), is up-regulated in many forms of cancer, as well as during cardiac hypertrophic growth. To understand its role, we overexpressed it in cardiocytes where it revealed a unique type of cell-to-cell "linker" in the form of long slender outgrowths and branches. We subsequently confirmed that miR-21 directly targets and down-regulates the expression of Sprouty2 (SPRY2), an inhibitor of branching morphogenesis and neurite outgrowths. We found that β-adrenergic receptor (βAR) stimulation induces up-regulation of miR-21 and down-regulation of SPRY2 and is, likewise, associated with connecting cell branches. Knockdown of SPRY2 reproduced the branching morphology in cardiocytes, and vice versa, knockdown of miR-21 using a specific 'miRNA eraser' or overexpression of SPRY2 inhibited βAR-induced cellular outgrowths. These structures enclose sarcomeres and connect adjacent cardiocytes through functional gap junctions. To determine how this aspect of miR-21 function translates in cancer cells, we knocked it down in colon cancer SW480 cells. This resulted in disappearance of their microvillus-like protrusions accompanied by SPRY2-dependent inhibition of cell migration. Thus, we propose that an increase in miR-21 enhances the formation of various types of cellular protrusions through directly targeting and down-regulating SPRY2.

INTRODUCTION

MicroRNA (miRNAs) are a newly discovered class of post-transcriptional regulators (Lagos-Quintana *et al*., 2002). An miRNA is ~22 ribonucleotides long, and genetically encoded, with a potential to recognize multiple mRNA targets guided by sequence complementarity and RNA-binding proteins (Lee *et al*., 1993). This class of molecules has the capacity to specifically inhibit translation or induce mRNA degradation, through predominantly targeting the 3′ untranslated regions (UTRs) of mRNA. miRNAs are differentially expressed during development and various diseases, thus implicating them in normal and pathological cellular mechanisms.

Although mammalian miRNAs are commonly known for inhibiting translation versus inducing mRNA degradation, there is now substantial evidence to support the latter as well. Farh *et al*. (2005) showed that predicted mRNA targets of tissue-specific miRNAs were lower in the corresponding tissue versus others. In support, Lim *et al*. (2005) showed that by expressing the muscle-specific miR-1 or the brain-specific miR-124 in HeLa cells, its mRNA expression pattern shifted accordingly. The mechanism of mRNA degradation is similar to that used by small interfering RNA (siRNA), where the endonuclease Dicer mediates mRNA cleavage. Alternatively, miRNA may induce deadenylation, which induces mRNA degradation (Wu *et al*., 2006). In contrast, it is well established that in metazoans miRNA inhibits mRNA translation, for which the Cap and poly(A) tail structures are required for inhibition of translation initiation, but the mechanism remains unknown (Humphreys *et al*., 2005). It is plausible that transient exposure of an mRNA to a targeting miRNA will inhibit its translation, whereas chronic exposure will result in its degradation.

miR-21 is one of the most commonly and highly up-regulated miRNA in many forms of cancer (Volinia *et al*., 2006; Meng *et al*., 2007). Its knockdown activates caspases and induces apoptosis in glioblastoma cells (Chan *et al*., 2005) and sensitizes cholangiocytes to chemotherapeutic agents (Meng *et al*., 2007), whereas its overexpression inhibits apoptosis in myeloma cells (Loffler *et al*., 2007). miR-21 is shown to target and down-regulate the expression of the tumor suppressors tropomyosin 1 (Zhu *et al*., 2007), phosphatase and tensin homologue (PTEN) (Meng *et al*., 2007), and programmed cell death 4 (Pdcd4) and promote cell invasion and metastasis (Asangani *et al*., 2007). Moreover, anti-miR-21 inhibits tumor growth in vivo and in vitro (Si *et al*., 2007). In human colorectal cancer, the levels of miR-21 positively correlated with the development of metastasis but not tumor size (Slaby *et al*., 2008). Most interestingly, of 37 differentially expressed miRNA (26 up-regulated and 11 down-regulated) in colon adenocarcinoma, up-regulation of miR-21 singularly correlated with lower survival rates and poor response of patients to therapy (Schetter *et al*., 2008). Thus, miR-21 is poised to be a major therapeutic target in colon carcinoma.

This article was published online ahead of print in *MBC in Press* (http://www.molbiolcell.org/cgi/doi/10.1091/mbc.E08–02–0159) on May 28, 2008.

† Present address: Department of Immunology, Merck & Co, Inc., 125 East Lincoln Avenue, Rahway, NJ 07065.

Address correspondence to: Maha Abdellatif (abdellma@umdnj.edu).

Cardiac hypertrophy is characterized by a change in the gene expression pattern that recapitulates the neonatal profile (Johnatty *et al*., 2000). This switch is triggered by transcriptional and post-transcriptional regulators. Several labs have recently reported an array of posttranscriptional miRNA regulators that are differentially expressed and play a role in the development of cardiac hypertrophy (van Rooij *et al*., 2006; Callis *et al*., 2007; Care *et al*., 2007; Cheng *et al*., 2007; Sayed *et al*., 2007; Tatsuguchi *et al*., 2007). miR-21 is one of the most highly and consistently up-regulated miRNAs, but its role is still controversial (Cheng *et al*., 2007; Tatsuguchi *et al*., 2007). The underlying mechanisms involved in cardiac hypertrophy are reminiscent of those used in cancer, overlapping in many growth-promoting molecules and pathways, wherein miR-21 proves to be no exception (van Rooij *et al*., 2006; Cheng *et al*., 2007; Sayed *et al*., 2007; Tatsuguchi *et al*., 2007).

In this study, we describe a role for miR-21 in inducing unique connections between cardiocytes, a morphological aspect of the cell that has not been described previously. We also identify an upstream regulatory pathway and a downstream target of miR-21. Their implications in cardiac hypertrophy and cancer are discussed.

MATERIALS AND METHODS

Transverse Aortic Constriction

C57Bl/6 were subjected to transverse aortic constriction as described previously (Sayed *et al*., 2007).

Cell Cultures and Adenovirus (Ad) Infection

Neonatal cardiocytes were prepared as described previously, using both preplating and Percoll gradients for enriching for cardiocytes (Abdellatif *et al*., 1994). Twenty-four hours later, medium was replaced without fetal bovine serum (FBS), and cells were infected with recombinant adenoviruses at a multiplicity of infection (moi) of 10–20.

Adult cardiocytes were prepared as described previously (Malhotra *et al*., 1997). Briefly, beating hearts were perfused in a Langendorf apparatus with collagenase type II (Worthington Biochemicals, Freehold, NJ) until cardiocytes were dissociated, and they were then cultured in minimal essential medium with 1.2 mM $CaCl_2$ on laminin-coated chamber slides.

Colon cancer SW480 and SW620 cell lines (American Type Culture Collection, Manassas, VA) were cultured in Leibovitz's medium (Invitrogen, Carlsbad, CA) with 10% FBS at 37°C in a CO_2-free incubator. Cells were infected with the various viruses in FBS-free medium.

Northern Blot

Total RNA extracted from whole hearts or cultured cardiocytes was analyzed by Northern blots as described previously (Sayed *et al*., 2007).

Construction of Adenoviruses

Recombinant adenoviruses were constructed, propagated, and titered as described previously by Dr. Frank Graham (Graham and Prevec, 1991). The viruses were purified on a cesium chloride gradient followed by dialysis against 20 mM Tris-buffered saline with 2% glycerol.

DNA Constructs Cloned into Recombinant Adenovirus

miR-21, a 320-base pair sequence encompassing the stem-loop of miR-21, was amplified from mouse genomic DNA by polymerase chain reaction (PCR) by using primers: 5′-CCTGCCTGAGCACCTCGTGC-3′ and 5′-GACTGTGACGACTACCCCAA-3′. For a control a nonsense sequence, 5′-GAACCGAGCCCACCAGCGAGC-3′ replaced the mature miRNA sequence within its stem-loop structure. An miR-21 eraser, a tandem repeat of the anti-sense of mature miR-21 sequence, was synthesized as a double-stranded oligonucleotide and cloned into recombinant adenovirus under the control of a U6 promotor. Sprouty2 (SPRY2; accession no. NM_011897, the full-length cDNA, excluding the miR-21 targeting site and upward of the 3′UTR, was cloned by PCR from a mouse 17-d embryonic cDNA library (Clontech, Mountain View, CA). Short hairpin RNA (shRNA) SPRY2, a hairpin-forming oligonucleotide corresponding to bases 668–688 of open reading frame of *Mus musculus* SPRY2 (GenBank accession no. NM_011897), was cloned into adenovirus as described previously (Yue *et al*., 2004).

Immunocytochemistry

As described previously (Sayed *et al*., 2007). Cells were immunolabeled with anti-titin (Developmental Studies Hybridoma Bank, University of Iowa, Iowa City, IA), anti-SPRY2 (Millipore, Billerica, MA), anti-connexin43 (Cx43; BD Biosciences, San Jose, CA), or anti-β-catenin (Santa Cruz Biotechnology, Santa Cruz, CA) in Tris-buffered saline with 1% bovine serum albumin. Slides were mounted using Prolong Gold anti-fade plus 4,6-diamidino-2-phenylindole (DAPI) (Invitrogen).

Immunohistochemistry

Slides were immunostained with 1:100 anti-connexin43 (BD Biosciences) by using BCIP/NBT chromagen from Zymed Laboratories (South San Francisco, CA), according to the manufacturer's protocol.

Cell Fractionation and Western Blotting

As described previously (Sayed *et al*., 2007), cell lysate was fractionated using Subcellular ProteoExtract kit (Calbiochem, San Diego, CA), according to the manufacturer's protocol. The protein (5–10 μg) was analyzed on a 4–20% gradient SDS-polyacrylamide gel electrophoresis (PAGE) (Criterion gels; Bio-Rad, Hercules, CA). The antibodies used were anti-SPRY2 and anti-SPRY3 (Millipore); anti-PDCD4, anti-SPRY1, anti-SPRY4, anti-Ras, and anti-H2B (Santa Cruz Biotechnology); anti-phospho-p44/42 mitogen-activated protein kinase (MAPK)-Thr202/Tyr204 and anti-p44/42 MAPK (Cell Signaling Technology, Danvers, MA); anti-connexin43 (BD Biosciences); anti-phosphatase and tensin homolog deleted on chromosome 10 (PTEN; GeneScript, Piscataway, NJ), and anti-glyceraldehyde-3-phosphate dehydrogenase (GAPDH; Millipore).

Luciferase (Luc) Assay

A concatemere of the miR-21–predicted target sequence within the SPRY2 3′UTR (GGAGACCCACATTGCATAAGCT) × 3 and a mutant lacking complimentarity with miR-21 seed sequence (GGAGACCCACATTGCGACTATA) × 3, were cloned downstream of the luciferase gene driven by the cytomegalovirus (CMV) promoter, generating Luc.SPRY2 and Luc.mtSPRY2 vectors, respectively. Cultured neonatal cardiocytes were transfected with these constructs, using Lipofectamine (Invitrogen), in conjunction with plasmids expressing miR-21 (CMV.miR-21) or a nonsense stem-loop (pControl). The cells were harvested after 24 h, and luciferase activity was assayed using an Lmax multiwell luminometer (Molecular Devices, Sunnyvale, CA).

Cell–Cell Dye Transfer Assay

A suspension of two groups (~10^5 cells) of freshly isolated neonatal cardiocytes were independently loaded with the gap junction-permeable dye calcein AM (0.5 μg/ml; Invitrogen) or with the membrane-labeling dye Vibrant DiI (1.86 μg/ml; Invitrogen), for 30 min at 37°C in serum-free culturing medium. The cells were then washed with 3 × 5 ml of medium and the two groups were mixed and plated on 0.3% gelatin-coated glass slide. Transfer of calcein from one group of cells to the other was monitored by live fluorescence imaging.

Migration Assay

SW480 cells were treated with a control, miR-21 eraser, shRNA-SPRY2, or miR-21 eraser + shRNA-SPRY2 viruses for 48 h in serum-free Leibovitz's medium, after which they were trypsinized, collected, and counted. In the meantime, 24-well plates with transwell-permeable, 0.8-μm polycarbonate membrane inserts (Corning, Corning, NY) were preconditioned with culture medium. To each transwell, 10^5 cells/100 μl of serum-free medium was seeded for 30 min before adding 600 μl of serum-enriched medium to the lower chamber as an attractant. The plates were incubated for 5 h at 37°C. The cells were then fixed with 10% buffered Formalin and kept at 4°C overnight, before they were stained with hematoxylin (Zymed Laboratories). The upper side of the membrane was gently wiped using a wet cotton swab to remove excess stain before the lower side was imaged with a 20× objective. The number of cells migrated were counted using the free ImageJ cell counter software (National Institutes of Health, Bethesda, MD).

Statistical Analysis

Calculation of significance between two groups was performed using an unpaired, two-tailed *t* test. The experiment in Figure 1e was performed twice, whereas all other experiments were done at least three times, as indicated in the figure legends. The relative intensities of the bands seen on Western blot or Northern blot radiographs were quantified using Unscan-it software and normalized to an internal control such as GAPDH, Ras, H2B, or actin for different cellular protein fractions, or U6 or 5S for RNA fractions. The numerical values reported within the text represent the average of at least three experiments ± SD. Otherwise, SE of the mean was used only where indicated in the text or figure legends.

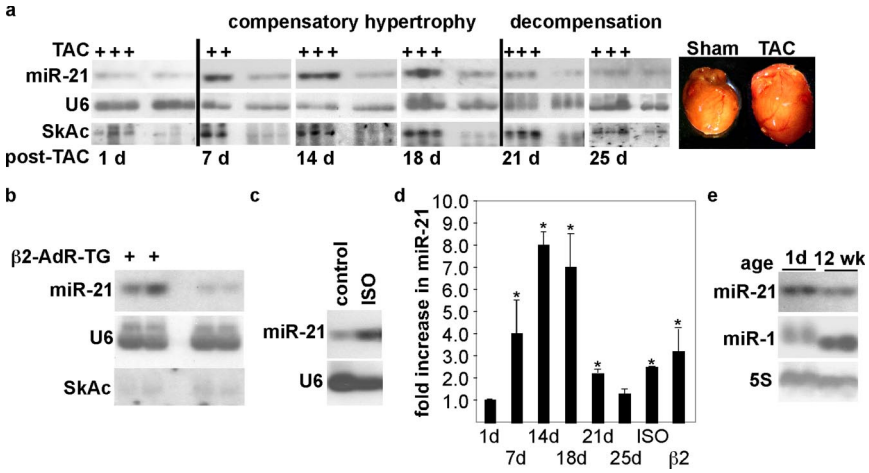

Figure 1. Mir-21 is up-regulated during cardiac hypertrophy. (a) Twelve-week-old male C57Bl/6 mice were subjected to TAC or a sham operation. Hearts were isolated 1, 7, 14, 18, 21, and 25 d post-TAC from which total RNA was extracted and analyzed by Northern blotting by using miR-21, U6, and skeletal actin detection probes (n = 3). The picture on the left shows the heart after 21 d of TAC versus sham operation. Reduced ejection fraction and increased left ventricular end diastolic pressure established the onset of cardiac decompensation (failure). (b) Total RNA was extracted from 1-y-old male β2AdR transgenic mice and their wild-type littermates and analyzed by Northern blotting (n = 4). (c) Cultured neonatal cardiocytes were treated with 10 μM isoproterenol (ISO) for 24 h, after which total RNA was extracted and analyzed by Northern blotting (n = 3). (d) The Northern blot signals for miR-21 were scanned, quantified, and normalized to the U6 signal. For each treatment or time point, average values are reported as -fold increase over control levels. Error bars represent SD, and *$p < 0.001$, TAC or growth factor versus sham or control. (e) Total RNA extracted from the hearts of 1-d and 12-wk-old rats was analyzed by Northern blotting using miR-21, miR-1, and 5S detection probes (n = 2).

RESULTS

miR-21 Is Up-Regulated during Cardiac Hypertrophy and through Stimulation of the β-Adrenergic Receptor

We have reported previously an array of microRNAs including miR-21 that was up-regulated during cardiac hypertrophy (Sayed *et al*., 2007). miR-21 increases by 4 ± 1.5- and 8.3 ± 0.6-fold (average ± SD; n = 3), at 7 and 14 d, respectively, after induction of hypertrophy by using transverse aortic constriction (TAC) versus a sham operation in a mouse model (Figure 1a). This was associated with 27 ± 6 and 35 ± 5% (average ± SD; n = 4) increase in heart and body weight, respectively, and an increase in skeletal actin, which is a marker of hypertrophy (Figure 1a). The increase in miR-21 was sustained through 18 d after TAC but started declining thereafter, concurrent with the onset of cardiac dysfunction (decompensation). We also assessed the levels of miR-21 in other genetic mouse models of cardiomyopathies, the results of which revealed its up-regulation in a transgenic mouse overexpressing β2-adrenergic receptor (β2AR) in the heart before development of any phenotype (Figure 1b). βAR stimulation plays a role in the development of cardiac hypertrophy, in which studies have shown that infusion of its agonist isoproterenol increases cardiac contractility and hypertrophy in rodent models. We further confirmed that isoproterenol induces up-regulation of miR-21 in isolated rat cardiocytes to almost the same extent as seen in the transgenic hearts (Figure 1, c and d). This suggests that the βAR receptors are upstream regulators of miR-21. miR-21, which is ubiquitously expressed in adult human and mouse tissue, is relatively low in the normal adult heart (Supplemental Figure 1S). It is developmentally regulated, which in contrast to the muscle specific miR-1 is higher in the neonatal heart that is known to grow though a process of cardiocyte hypertrophy (Figure 1e). Thus, an increase in miR-21 accompanies hypertrophic growth, with the βAR receptor being one of its upstream regulators.

miR-21 Targets Sprouty2 and Induces Cellular Outgrowths

To address the role of miR-21 in cardiocytes, we cloned a 320-nt sequence that encompasses the miR-21 stem-loop into a recombinant adenovirus (Figure 2a). We similarly cloned a tandem repeat of the antisense sequence of mature miR-21 under the control of the U6 promoter (Figure 2b). Northern blots analysis of cardiocytes treated with the former vector exhibit approximately threefold higher mature miR-21 versus control, although the premature construct accumulated at much higher levels, reflecting a rate-limiting step in the processing of miR-21 (Figure 2a). In contrast, the antisense miR-21 was highly expressed and resulted in knockdown of endogenous miR-21, but not miR-1, where it was undetectable by Northern blotting (Figure 2b). For that reason, we dubbed this construct miR-21 eraser. The function of this eraser was further validated in SW480 and SW620 cancer cells with regard to the established miR-21 targets, programmed cell death 4, and PTEN (Supplemental Figure 2S, Ad). We also established the specificity and versatility of these erasers by showing that an "miR-199a eraser" specifically eliminated the corresponding miRNA but not miR-21 or miR-1 (Supplemental Figure 2S, E).

Overexpressing miR-21 in cardiocytes did not influence hypertrophic growth in the absence or presence of growth factors as monitored by [^{3}H]leucine incorporation (data not shown). But after 48–72 h in culture, we noticed all the cells exhibited extensive cellular outgrowths (4 ± 3 branches/cell, average ± SD; n = 25) that varied in length (44 ± 28 μm, average ± SD; n = 25) depending on the distance between neighboring cells (Figure 2c). Sprouty, a known inhibitor of branching morphogenesis and neurite outgrowth, is predicted to be a miR-21 target by TargetScanS and PicTar miRNA target prediction software, each using a unique set of algorithms. To confirm its potential in mediating the branching effects of miR-21, we independently knocked it down using adenoviral delivered short-hairpin RNA (Figure 2f). This elicited even more impressive cardiocyte outgrowths (Figure 2c). Neither miR-21 nor the shRNA against SPRY2 had any effect on SPRY1, -3, or -4 (Supplemental Figure 3S). Furthermore, overexpression of SPRY2 inhibited miR-21-induced outgrowths (Figure 2d), which suggested that the effect of miR-21 is mediated through this putative target.

Using Western blot analysis, we confirmed down-regulation of endogenous SPRY2 (52 ± 4%, average ± SD; n = 4) upon overexpression of miR-21 for 48 h (Figure 2e). The

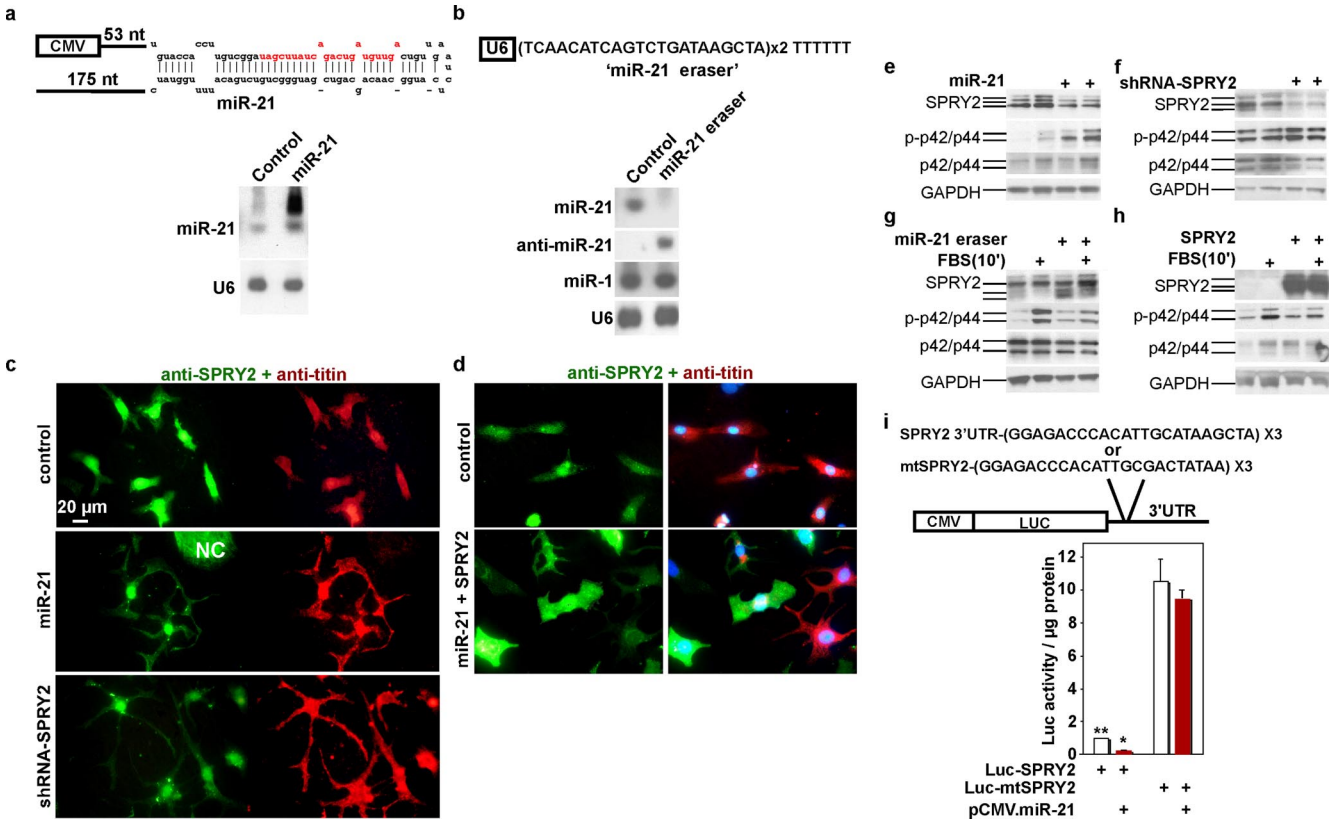

Figure 2. miR-21 induces cardiocyte outgrowth and down-regulation of SPRY2. (a) The stem-loop structure of miR-21 under the control of the CMV promoter cloned into recombinant Ad, in which the mature sequence is shown in red. (b) The anti-miR-21 (miR-21 eraser) sequence under the control of the U6 promoter cloned into recombinant adenovirus. The panels below each construct represent Northern blots of RNA extracted from cardiocytes infected with 10–20 moi of the corresponding virus for 48 h (n = 3). (c) Cardiocytes cultured on uncoated glass chamber slides were infected with 10–20 moi of adenovirus expressing miR-21 (n = 20) or short hairpin SPRY2 (shRNA-SPRY2) in serum-free medium (n = 6). (d) Similarly cells were treated with 10–20 moi of control or a combination of miR-21 and SPRY2 Ad viruses (n = 4). Seventy-two hours later, cells were fixed and coimmunolabeled with anti-SPRY2 (green), anti-titin (red), and DAPI (blue). Cells were imaged with an epifluorescence microscope at 60× magnification by using an fluorescein isothiocyanate (FITC) (green), Texas Red (red), or FITC/Texas Red/DAPI triple filter, as shown. NC, noncardiac cell. (e–h) Cardiocytes were infected with Ad expressing miR-21 (n = 4; e), shRNA-SPRY2 (n = 4; f), miR-21 eraser (n = 4; g), or SPRY2 (n = 4; h) and control Ad expressing scrambled miR, or lacz, respectively, for 48 h, in serum-free medium, as marked with the + sign. Cells were additionally treated with 10% FBS for 10 min, where indicated. Control lanes (unmarked with +) were treated with a scrambled stem-loop– (e–g) or a Lacz (h)—expressing virus. Cells were harvested, and the cytosolic fraction was analyzed by Western blotting using anti-SPRY2, anti-phosoho-p42/p44 (p-p42/p44), anti-p42/p44, anti-GAPDH, and anti-α sarcomeric actin (s.actin). (i) Cardiocytes were transfected with a CMV.Luc vector containing the predicted miR-21 target sequence in SPRY2 (Luc-SPRY2) or a control mutated sequence (Luc-mtSPRY2), within the 3′UTR of Luc, where indicated by the + sign. In conjunction, cells were cotransfected with plasmids expressing miR-21 (red bars) or a control nonsense stem-loop sequence (open bars). After 24 h, protein was extracted, and luciferase activity per microgram of protein was measured and averaged (n = 12). The results are graphed as -fold increase in luciferase activity relative to Luc-SPRY2 in the absence of miR-21 after adjusting it to 1. Error bars represent SE of the mean, and *$p < 0.001$, Luc-SPRY2 + miR-21 versus Luc-SPRY2 alone; **$p < 0.0001$, Luc-SPRY2 versus Luc-mtSPRY2.

blots also revealed that the SPRY2 protein is present in the cytosol, membrane, nuclear, and cytoskeletal fractions of cardiocytes (Supplemental Figure 4S). It should be noted that SPRY2 is detected as two to three bands on an SDS-PAGE, which is thought to be due to its phosphorylation and palmitoylation (Impagnatiello *et al*., 2001). The quantification takes into account all three forms. In contrast, overexpression of SPRY2 had no effect on endogenous miR-21 (Supplemental Figure 5S). Because Sprouty negatively regulates extracellular signal-regulated kinase (ERK)1/2, we used phospho-ERK1/2 as a marker for monitoring changes in Spry2 function that would be regulated by changes in its levels. The results show that down-regulation of SPRY2 by miR-21 or shRNA (67 ± 9%, average ± SD; n = 4) is accompanied by an increase in basal phosph-ERK1/2 normalized to the total ERK by 5 ± 0.4 (average ± SD; n = 4) and 2.2 ± 0.15-fold (average ± SD; n = 4), respectively (Figure 2, e and f). But excess (overexpressed) miR-21 did not augment FBS-induced phospho-ERK1/2 levels; plausibly, FBS has already induced maximal stimulation (Supplemental Figure 4SB). The increase of phospho-ERK1/2 by these treatments may reflect the inhibitory effect of SPRY2 on basal activation of surface receptors through autocrine effects. In contrast, knockdown of miR-21 by using the miR-21 eraser, or overexpression of SPRY2, results in >80% inhibition of fetal bovine serum-induced phospho-ERK1/2 (Figure 2, g and h). Thus, SPRY2 is a downstream target of miR-21 (could be a direct or indirect target at this juncture) and has limiting cellular concentrations.

To determine whether SPRY2 is a direct target of miR-21, we cloned the miR-21–predicted target sequence that is contained within its 3′UTR, downstream of a luciferase gene (Luc.SPRY2; Figure 2i). This sequence conferred miR-21–induced inhibition of the luciferase activity by

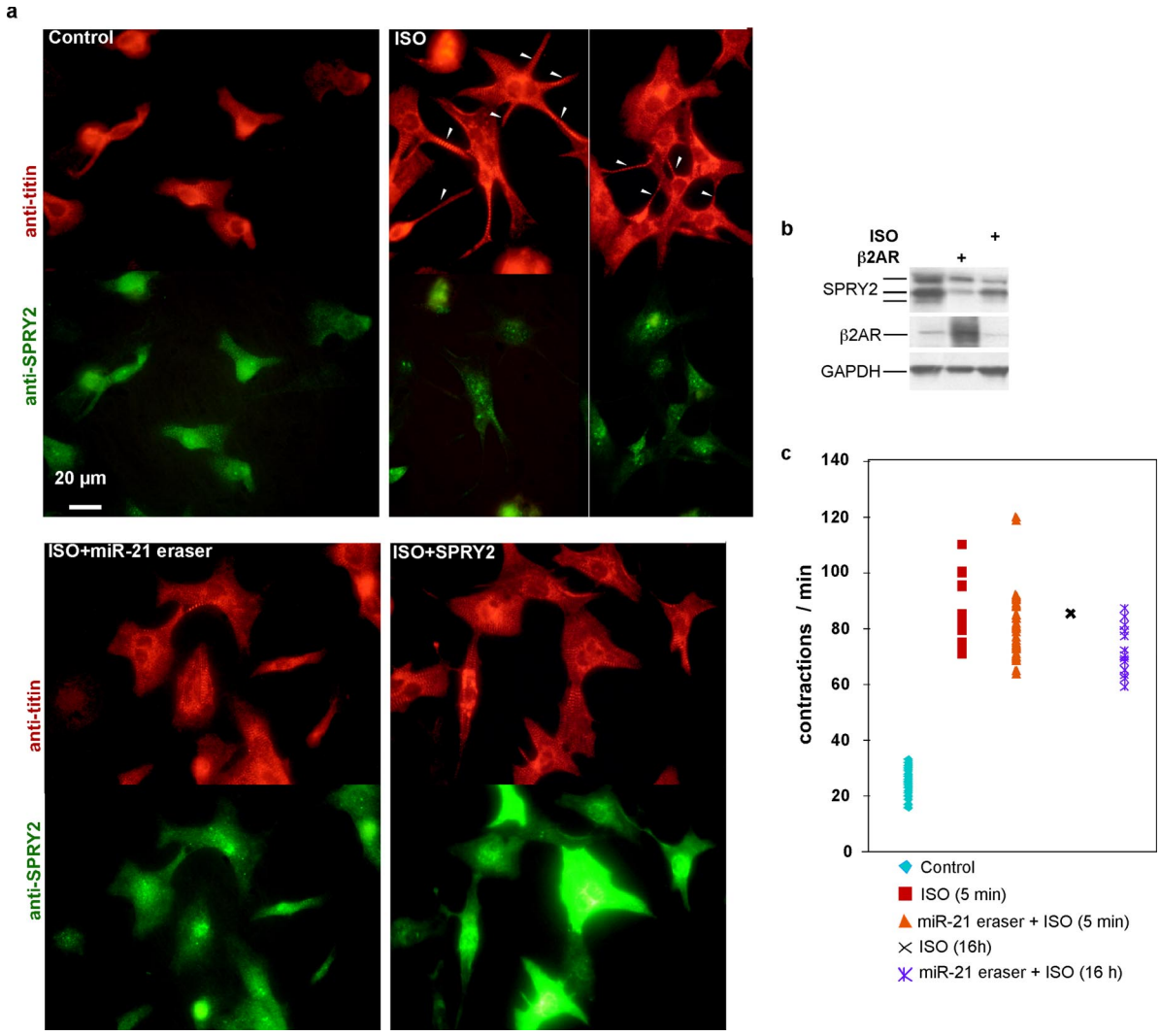

Figure 3. β-Adrenergic receptors induces cellular outgrowths and down-regulation of SPRY2 in cardiocytes. (a) Cardiocytes cultured on uncoated chamber slides were treated with 10 μM isoproterenol (ISO) in the presence or absence of 10–20 moi of Ad expressing miR-21 eraser or SPRY2, in serum-free medium (n = 3). After 24 h, cells were fixed and coimmunostained with anti-titin (red) and anti-SPRY2 (green). Cells were imaged with an epifluorescence microscope at 60× magnification. Arrowheads point to connecting branches. (b) Cardiocytes were treated with 10 μM ISO or 10–20 moi of Ad expressing β2-AR, in serum-free medium (n = 3). After 24 h, cells were harvested, and the cytosolic fraction was analyzed by Western blotting by using anti-SPRY2, anti-β2AdR, and anti-GAPDH. (c) Cardiocytes were treated with 10–20 moi of Ad.miR-21eraser in serum-free medium. After 24 h, they were stimulated with 10 μM ISO. Beats/min for 10–20 cells/field (n = 3) were counted after 5 min or 16 h of addition of the drug. The results are presented as beats per minute for each cell under the conditions indicated in the legend.

76 ± 4% (average ± SEM; n = 12). To determine specificity, we cloned a mutated miR-21 SPRY2 target sequence, in which the seed-binding sequence was completely altered (Luc.mtSPRY2), downstream of the luciferase gene. As seen in Figure 2i, not only did this mutant abolish the effect of exogenous miR-21 on the reporter but also it relieved it from inhibition by the endogenous miR-21. Thus, we conclude that SPRY2 is a direct target of miR-21.

β-Adrenergic Receptor Stimulation Induces down-Regulation of SPRY2, Which Is Accompanied by Cell-to-Cell Connecting Cellular Outgrowths

To address physiological relevance of these miR-21–induced outgrowths, we asked whether these structures accompany βAR induction of miR-21 in isolated cardiocytes. After treatment of the cells with isoproterenol and staining them with an antibody against the sarcomeric protein titin, we were able to observe cellular outgrowth that were connecting or reaching out to adjacent cells (Figure 3a, top). The striated pattern of titin staining reflects the presence of sarcomeres even within these branches. This effect was wide spread in all observed cells (4 ± 3 branches/cell, average ± SD; n = 20). Impressively, these outgrowths were abrogated by the miR-21 eraser or overexpression of SPRY2 (Figure 3a, bottom). Coimmunostaining the cells with anti-SPRY2 reveals that SPRY2 is depressed in the presence of isoproterenol but restored in the presence of the miR-21 eraser or exogenous SPRY2. Similar results were obtained when cells were treated with a virus overexpressing β2AR (Supplemental Figure 6S). Although Figure 1 confirms that isoproterenol and β2AR induce up-regulation of miR-21, Figure 3b confirms that they also induce 70 ± 22 and 64 ± 11 (average ±

SD; n = 3) down-regulation of SPRY2 protein, respectively (Figure 3b). The functional consequence of this effect is reflected in the contractile behavior of the cardiocytes (Figure 3c). Normally, isolated cells have variable beating rates. In the presence of isoproterenol, the rate of contraction is immediately enhanced two- to fivefold and does not seem to suffer in the absence of miR-21. But after 24 h of stimulation, the cardiocytes are hypertrophied and form cell-to-cell connections and begin to beat synchronously. By disrupting the connecting cellular outgrowth, using miR-21 eraser, this synchronicity of beating is disrupted. Thus, cell-to-cell connecting cardiocyte outgrowths are a morphological change that accompanies βAR stimulation and hypertrophy and that is mediated by miR-21 through down-regulation of SPRY2. From the contractile behavior of the cells, we predicted that these outgrowths connect the cardiocytes via functional gap junctions, which we test next.

Cellular Outgrowths Connect to Cardiocytes via Gap Junctions

To verify the type of cell–cell connections conferred by these outgrowths, we immunostained Ad.miR-21- or isoproterenol-treated cardiocytes with anti-Cx43 and anti-β-catenin for detection of gap or adherens/tight junctions, respectively. Our results show that isoproterenol treatment (Figure 4a, bottom), relative to control (Figure 4a, top), induced interconnecting branches accompanied by redistribution of Cx43 and β-catenin that became distinctly localized at branch-to-cell contact points. It seems that Cx43 alone is more prevalent at these connections (white arrowheads), where β-catenin was occasionally found to coexist (yellow arrowheads). Although miR-21 induced a similar effect, the redistribution of Cx43 and β-catenin at the connection sites was less pronounced (Figure 4a, middle). This led us to conclude that isoproterenol induces additional factors that enhance the formation of gap junctions.

To test the functionality of these gap junction connections, we coplated two groups of cardiocytes, one group loaded with cytosolic calcein AM (green) and the other group labeled with the membrane dye Vybrant DiI (red). This approach enables us to distinguish any cells that might acquire calcein AM de novo from the originally loaded cells. Although the untreated cells show two distinct single-color populations, after treatment with isoproterenol we could identify Vybrant DiI-labeled cells (red arrowheads) that had acquired the green dye from an adjacent calcein-only positive cell (white arrowheads), in which the transferring dye could also be seen in the connecting branch (Figure 4b). Thus, interconnecting cardiocyte branches serve the purpose of conduction of molecules between cells.

Because the experiments described above were performed in neonatal cultured cardiocytes, which are generally more plastic, we questioned how these outgrowths might develop in the morphologically uniform rod-shaped adult cardiocytes in vivo. For this purpose, we sectioned hypertrophied hearts from the TAC mouse model and immunostained them with anti-Cx43. Compared with normal hearts, these hearts showed connecting, short, lateral outgrowths between adjacent cardiocytes, in which Cx43 that is normally strictly localized to the intercalated discs demarcated the sites of contact (Figure 5a). The figure shows three different depictions of these connections. To determine whether miR-21 mediates this effect, we isolated normal adult cardiocytes that we treated with the miR-21–expressing adenovirus for 72 h. After immunostaining with anti-Cx43, we were able to observe Cx43-demarcated lateral protrusions (Figure 5b, arrowheads). We also determined

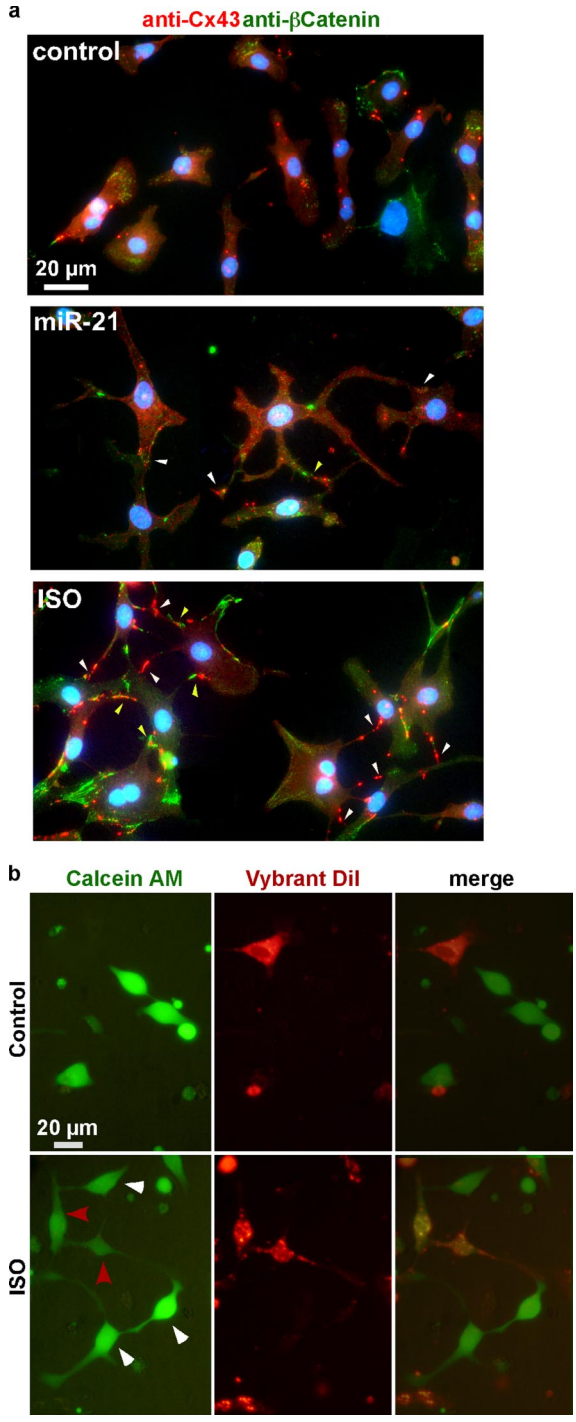

Figure 4. Cardiocyte outgrowths connect cells via gap junctions. (a) Neonatal cardiocytes cultured on uncoated chamber slides were treated with 10–20 moi of Ad expressing miR-21 for 48 h or 10 μM ISO for 24 h (n = 3). Cells were then fixed and coimmunolabeled with anti-Cx43 (red) and anti-β-catenin (green) and DAPI (blue). NC, noncardiac cell. Cells were imaged with an epifluorescence microscope at 60× magnification by using an FITC/Texas Red/DAPI triple filter. Arrowheads point to the connection sites of branches. (b) Two populations of neonatal cardiocytes were separately loaded with calcein AM (green) or Vybrant DiI (red) before coculturing for 16 h (n = 3). Cells were then treated with 10 μM ISO for 8 h followed by live imaging at 40× magnification. White arrowheads point to cells loaded with calcein only; red arrowheads point to cells that were loaded with Vybrant DiI only but have acquired calcein through the connecting branches.

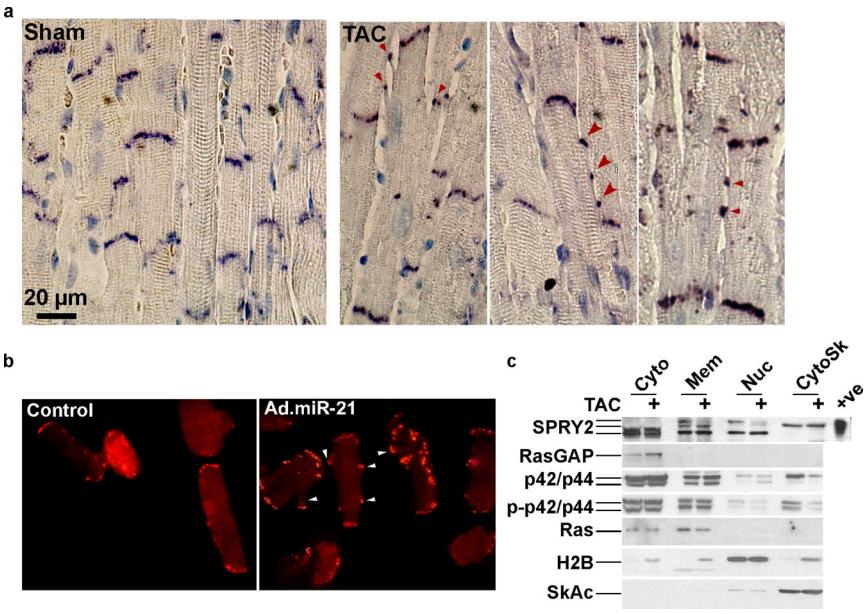

Figure 5. Cardiac hypertrophy is associated with connexin43 positive side-branch connections and down-regulation of SPRY2. (a) Twelve-week-old male C57Bl/6 mice were subjected to TAC. Two weeks later, the hearts were isolated fixed, sectioned, and immunostained with anti-Cx43 (dark purple) and counterstained with hematoxylin (blue nuclei; n = 3). Arrowheads point to connecting side branches. (b) Adult rat cardiocytes were cultured on laminin-coated chamber slides. The cells were then infected with 20–40 moi of Ad expressing miR-21 or a control scrambled sequence (n = 3). After 48 h, they were fixed and immunolabeled with anti-Cx43 (red). Cells were imaged with an epifluorescence microscope at 60× magnification. (c) From hearts similar to those described in a, cellular protein was extracted; fractionated into cytoplasm (Cyto), membrane (Mem), nuclei (Nuc), and cytoskeleton (CytoSk); and analyzed by Western blotting using anti-SPRY2, anti-Ras GTPase-activating protein (RasGAP), anti-p-p42/p44, and anti-p42/p44 (n = 3). Anti-Ras, anti-histone H2B, and anti-skeletal actin (SkAc) are used to validate the membrane, nuclear, and sarcomeric fractions, respectively, whereas anti-RasGAP validates the cytosolic fraction.

the levels of SPRY2 in the hypertrophied heart. The change in SPRY2 protein was only detected in the slower migrating form (~90%; n = 3), both in the membrane and nuclear fractions, but it was not associated with an increase in phosph-ERK1/2 (Figure 5c). Thus, the up-regulation of miR-21 in the adult cardiocytes evokes a rudimentary form of the cellular outgrowths observed in the neonatal cardiocytes.

miR-21 Mediates the Formation of Microvillus-like Protrusions in Colon Cancer Cells

miR-21 is overexpressed in many cancer forms. To determine how the effect of miR-21 seen in cardiocytes translates in cancer cells, we overexpressed miR-21, SPRY2, or miR-21 eraser, in the colon cancer cells SW480. Overexpression of miR-21 results in a minimal increase over the already very high endogenous levels, whereas miR-21 eraser results in ~70% (n = 2) reduction in endogenous miR-21 (Figure 6a) accompanied by up-regulation of SPRY2 protein (Figure 6c). Staining the cells with actin-binding phalloidin reveals microvillus-like protrusions that are enriched throughout the circumference of the control and miR-21–overexpressing cells alike (Figure 6b). In contrast, SPRY2 and miR-21 eraser resulted in dramatic reduction of these protrusions. Immunostaining the cells confirmed an increase in SPRY2 accompanying miR-21 eraser or SPRY2 overexpression. In addition to a reduction of the microvilli-like structures, miR-21 knockdown was associated with a 0.4 ± 0.12-fold lower cell migration relative to control, which was almost completely rescued by shRNA-SPRY2 (Figure 6c). Conversely, shRNA-SPRY2 alone increased cell migration 1.47 ± 0.05-fold that was inhibited by miR-21 eraser. Western blot analysis demonstrates the corresponding changes in SPRY2 levels, which reflects its increase with miR-21 eraser, inhibition by shRNA-SPRY2, and its inverse correlation with the extent of migration. Thus, we conclude that miR-21, through inhibition of SPRY2, reduces the formation of microvillus-like protrusions and migration of colon cancer cells.

DISCUSSION

miR-21, Its Association with Cell Growth and Its Upstream Regulators

miR-21 has attracted more attention than any other miRNA, because it is one of the most highly up-regulated in various cancers, cardiac hypertrophy, and neointimal formation, suggesting that it has a fundamental role in cell growth. In agreement, its level is fairly higher in the neonatal versus adult heart (Figure 1e), where it is up-regulated upon induction of hypertrophic growth. In contrast, its level starts declining with the onset of cardiac failure, ultimately dropping to basal amounts. This also coincides with down-regulation and desensitization of the βARs (Bristow *et al*., 1982). Moreover, β2AR-overexpressing mice exhibit up-regulation of miR-21 in the heart, whereas isoproterenol stimulation of cultured cardiocytes induces up-regulation of miR-21, down-regulation of SPRY2, and enhanced myocyte branching. Collectively, these data suggest that βARs are upstream regulators of miR-21 in the heart. Interestingly, it was recently reported that stress mediated through βAR stimulation enhances ovarian cancer cell invasiveness (Sood *et al*., 2006). Thus, it is also plausible that βAR also plays a role in enhancing miR-21 in cancer cells, where it may induce up-regulation of miR-21, down-regulation of SPRY2, and increased microvillus-like protrusions, and thereby cell migration.

Evidence Supporting a Role for βAR in Inducing Cardiocyte Connectivity and Its Association with Cardiac Hypertrophy

In support of a role for βAR stimulation in cell–cell connections and conduction, it was recently reported to increase the expression of connexin43 (Salameh *et al*., 2006) and conduction velocity in cultured neonatal cardiocytes (de Boer *et al*., 2007). Conduction velocity, which is partly regulated by the abundance of gap junctions, is increased during early hypertrophy but decreased during later decompensation stages (Cooklin *et al*., 1998), which coincides with the decline in βARs and connexin43. Similarly, stretch (Zhuang *et al*.,

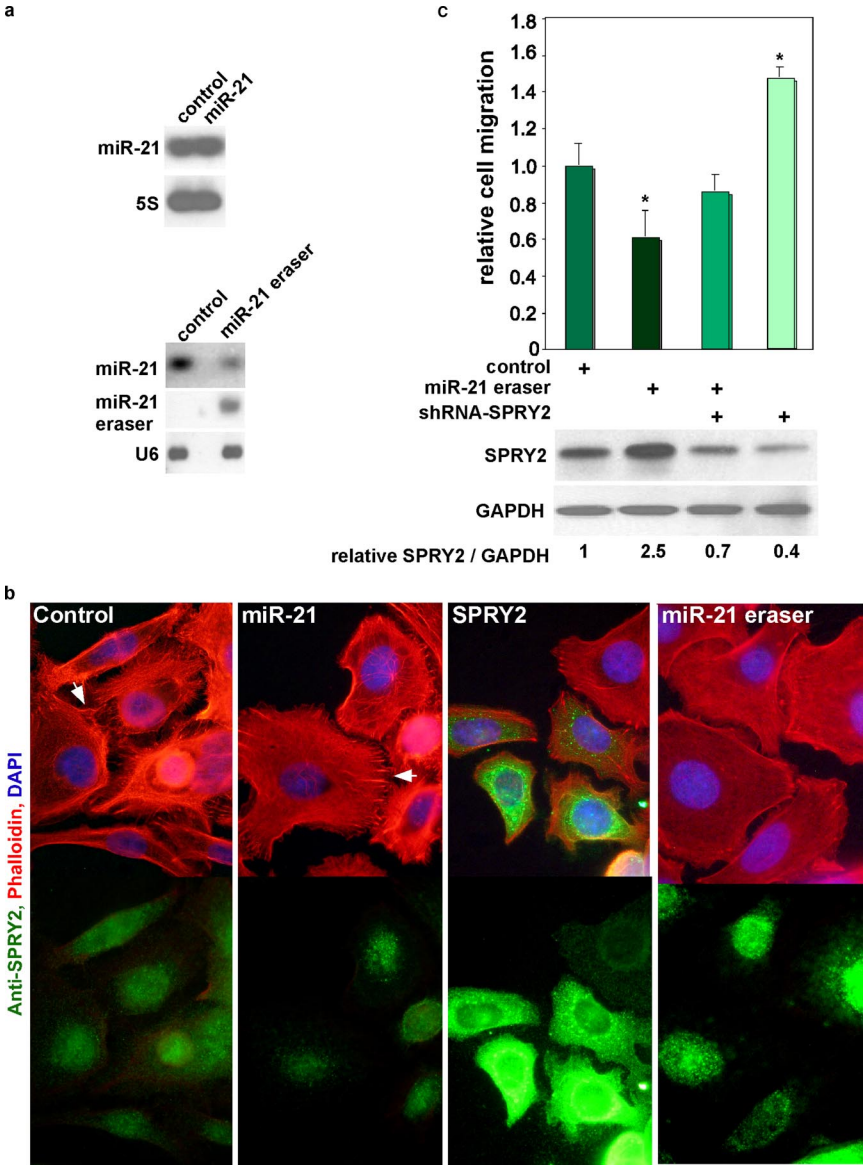

Figure 6. Overexpression of SPRY2 or knockdown of miR-21 in colon cancer cells reduces the formation of microvillus-like protrusions and cell migration. (a) SW480 cells were treated with Ad expressing miR-21 (top) or miR-21 eraser (bottom). Forty-eight hours later, total RNA was extracted and analyzed by Northern blotting by using miR-21, miR-21 eraser, 5S, or U6 detection probes (n = 2). (b) SW480 cells cultured on glass chamber slides were infected with Ad expressing miR-21, SPRY2, or miR-21 eraser (moi 20 each) in serum-free medium (n = 3). After 48 h, cells were fixed and immunolabeled with anti-SPRY2 (green) and phalloidin (red). Cells were imaged with an epifluorescence microscope at 60× magnification by using a FITC/Texas Red/DAPI triple or just FITC (green) filter, as shown. Arrows point to microvilli-like protrusions. (c) Cells were treated with a control virus, miR-21eraser, shRNA-SPRY2, or miR-21 eraser + shRNA-SPRY2 for 48 h in serum-free Leibovitz's medium, after which they were trypsinized, collected, and counted. For the migration assay, 10^5 cells were seeded on transwell filters with 0.8-μm pores, for 30 min, before the addition of 600 μl of serum-enriched medium to the lower chamber (n = 9). After 5 h, cells were fixed, stained, imaged with an 80× objective, and counted on the bottom side of the filter from three fields/well by using the ImageJ cell counter software (National Institutes of Health). The difference in cell migration seen with the various treatments was calculated as -fold change relative to the control treatment after adjusting it to 1, and data are plotted as a bar graph, with error bars representing SE of the mean and asterisks (*) representing $p < 0.001$, calculated for miR-21eraser- or shRNA-SPRY2- versus control-treated cells. Protein extracts from similarly treated cells were analyzed by a Western blot for SPRY2, which is displayed below the graph (n = 2).

2000) and cAMP (Darrow *et al*., 1996) induce up-regulation of connexin43 and gap junction density in parallel with an increase in conduction velocity in cultured cardiocytes. These data reconcile well with our results in Figure 3a showing extensive interconnecting cellular branches induced by isoproterenol treatment of isolated cardiocytes.

Cardiocytes adjacent to infarct zones (Smith *et al*., 1991) or those subjected to aortic banding-induced hypertrophy (Emdad *et al*., 2001) or pulmonary hypertension-induced hypertrophy (Uzzaman *et al*., 2000) exhibit extensive remodeling of gap junctions. This remodeling is in the form of punctate distribution of connexin43 throughout the perimeter of the cell, which is normally confined to its end intercalate discs. This is similar to its diffuse distribution in neonatal heart cardiocytes (Spach *et al*., 2000). Interestingly, we observe a similar pattern of connexin43 labeling after TAC and in isolated adult cardiocytes overexpressing miR-21 (Figure 5b). We propose that the lateralization of connexin43 demarcates sites of cell-to-cell connecting branches, which are induced by up-regulation of miR-21 and down-regulation of its target SPRY2. Similarly, in normal human hearts connexin43 is predominantly (91.7%) restricted to the intercalated discs (Kostin *et al*., 2004). During early stages of cardiac hypertrophy, connexin43 is increased by 44.3%, but only 60.3% is localized to intercalated discs, whereas more of the protein occurs on the lateral sarcolemma (Kostin *et al*., 2004). But during later stages of hypertrophy and decompensation, connexin43 levels are reduced and the lateral distribution disappears. This distribution and expression profile of connexin43 agrees with a scenario in which increased miR-21 during compensatory hypertrophy is associated with increased Cx43-positive, cell-cell connecting side branches, which is reversed during failure commensurate with the decline of miR-21.

The Role of SPRY in Branching and Cancer

Sprouty was first discovered as an inhibitor of fibroblast growth factor (FGF) signaling and branching of *Drosophila* airways (Hacohen *et al*., 1998). This effect is conserved as shown by knockdown of SPRY2 in mouse lungs (Tefft *et al*., 1999). Sprouty inhibits MAPK activation by FGF and epidermal growth factor (Reich *et al*., 1999). Inhibition of

branching is not restricted to the lungs, but SPRY2 also inhibits ureteric (Chi *et al*., 2004) as well as chorionic vellous branching and reduces trophoblast cell migration (Chi *et al*., 2004). Although the branches referred to here are tubular multicellular structures that underlie organogenesis, they are initiated by single cell sprouting. But most relevant to our study, is inhibition of neurite outgrowths by SPRY2 (Lao *et al*., 2006; Gross *et al*., 2007).

A related isoform, SPRY1, was reported to be up-regulated after relieving a human heart from its workload, which is consistent with our finding in which SPRY2 is down-regulated during pressure overload (Huebert *et al*., 2004). SPRY was also found in vascular endothelial cells and has been shown to inhibit vasculogenesis (Huebert *et al*., 2004). Likewise, Sprouty4 inhibits FGF and vascular endothelial growth factor-induced endothelial cell migration and proliferation (Lee *et al*., 2001), whereas SPRY2 inhibits migration and proliferation of smooth muscle cells (Zhang *et al*., 2005). This reconciles well with the observed up-regulation of miR-21 during neointimal formation, which has been shown to enhance smooth muscle proliferation (Ji *et al*., 2007), and our discovery of SPRY2 being one of its targets.

Sprouty is down-regulated in prostrate cancer (Kwabi-Addo *et al*., 2004), breast cancer (Lo *et al*., 2004), hepatocellular carcinoma (Fong *et al*., 2006), and non–small-cell lung cancer (Sutterluty *et al*., 2007). Although independently, it was shown that these forms of cancer are also associated with up-regulation of miR-21 (Volinia *et al*., 2006; Meng *et al*., 2007). Whereas overexpression of SPRY2 inhibits cell migration (Yigzaw *et al*., 2001; Lee *et al*., 2004), an increase in miR-21 enhances cell proliferation and migration (Meng *et al*., 2007). This is consistent with a pathway in which up-regulated miR-21 targets and down-regulates SPRY2, thereby enhancing proliferation and migration. But in addition, it has been shown that miR-21 can contribute to carcinogenesis through inhibition of apoptosis, or down-regulation of other tumor suppressors, such as phosphatase and PTEN (Meng *et al*., 2007) and tropomyosin 1 (Zhu *et al*., 2007). This further establishes a link between miR-21 and SPRY2, which is known to induce up-regulation of PTEN and inhibit cell proliferation (Edwin *et al*., 2006). Using the miR-21 eraser in cancer cells, we show that knockdown of miR-21 is associated with up-regulation of both SPRY2 and PTEN. Thus, it seems that miR-21 negatively regulates PTEN both directly and indirectly through inhibition of SPRY2. Moreover, SPRY2 differentially regulates apoptosis: in differentiated neuronal cells it is apoptotic (Gross *et al*., 2007), but it is antiapoptotic in adenocarcinoma cells (Edwin and Patel, 2008). Our results suggest that miR-21 through down-regulating SPRY2 enhances migration through promoting formation of microvillus-like protrusions. But, the possibility remains that miR-21 through inhibition of SPRY2 and PTEN enhances cancer cell proliferation as well. Also, while validating the function of our miR-21 eraser, we found that it up-regulates PDCD4 in SW480 but not in myocytes, corroborating an antiapoptotic effect of miR-21 in cancer cells.

The Eraser Is a Powerful Tool for Specific Knockdown of Endogenous miRNA

Inhibition or knockdown of a specific miRNA is key in understanding its function. For that purpose several approaches have been devised. Those include the 2′-*O*-methyl (Hutvagner *et al*., 2004; Meister *et al*., 2004) or LNA-modified oligoribonuleotides (Orom *et al*., 2006), and "antagomirs," which have a phosphorothioate backbone, a cholesterol-moiety at 3′ end, and 2′-*O*-methyl modifications (Krutzfeldt *et al*., 2005). In contrast to these transiently delivered oligonucleotides, Ebert *et al*. (2007) have recently reported the delivery of antisense miRNA sequence by using expression vectors termed "sponges" (Ebert *et al*., 2007). Our miRNA eraser is similar in concept to the latter, but it differs in the mechanism of inhibition of the miRNA. Although the sponges induce a modest variable decrease of the endogenous miRNA, our eraser wipes it out. The apparent loss of the miRNA signal on the Northern blots cannot be explained by competition of the complementary eraser RNA with the labeled miRNA probe used for the detection, as proposed by Ebert *et al*. (2007) because Northern blots are normally run under extreme denaturing conditions. In cardiocytes, miR-specific erasers rendered endogenous miR-21 and miR-199a undetectable on Northern blots. In colon cancer cells, however, the effect was less complete only because it was diluted out by the rapidly proliferating cultures. The eraser differs from the sponge in two physical aspects: 1) the lack of stem-loop sequences at the 5′ and 3′ ends of tandem repeat sequence and 2) its delivery via a viral vector. Other plausible reasons for the difference in the outcome are the nature of the cell types or the targeted microRNA tested in both studies.

In conclusion, miR-21 plays a role in inducing the formation of cellular outgrowths that connect cardiocytes through gap junctions, which are usually confined to the intercalated discs in the normal adult heart. This change is provoked by βAR stimulation and mediated through down-regulation of SPRY2, an established negative regulator branching morphogenesis. We propose that this is an adaptive effect seen during cardiac hypertrophic growth and that it is associated with gap junction remodeling and enhanced conduction velocity but that it is reversed during cardiac failure. In contrast, miR-21 is necessary for formation of microvillus-like protrusions in colon cancer cells and enhances cell migration. It remains to be tested whether βAR stimulation also induces up-regulation of miR-21 in cancer cells, which if confirmed would provide us with a convenient therapeutic target.

ACKNOWLEDGMENTS

We thank Dr. Stephen F. Vatner (Department of Cell Biology and Molecular Medicine) for advice and support. This work was supported in part by the National Institutes of Health grants 2R01 HL-057970-06 and 1R01 HL-081381-01A1 (to M. A.).

REFERENCES

Abdellatif, M., Mcllelan, W. R., and Schneider, M. D. (1994). p21 Ras as a governer of global gene expression. J. Biol. Chem. *269*, 15423–15426.

Asangani, I. A., Rasheed, S. A., Nikolova, D. A., Leupold, J. H., Colburn, N. H., Post, S., and Allgayer, H. (2007). MicroRNA-21 (miR-21) post-transcriptionally downregulates tumor suppressor Pdcd4 and stimulates invasion, intravasation and metastasis in colorectal cancer. Oncogene *29*, 29.

Bristow, M. R., Ginsburg, R., Minobe, W., Cubicciotti, R. S., Sageman, W. S., Lurie, K., Billingham, M. E., Harrison, D. C., and Stinson, E. B. (1982). Decreased catecholamine sensitivity and beta-adrenergic-receptor density in failing human hearts. N. Engl. J. Med. *307*, 205–211.

Callis, T. E., Chen, J. F., and Wang, D. Z. (2007). MicroRNAs in skeletal and cardiac muscle development. DNA Cell Biol. *26*, 219–225.

Care, A. *et al*. (2007). MicroRNA-133 controls cardiac hypertrophy. Nat. Med. *13*, 613–618.

Chan, J. A., Krichevsky, A. M., and Kosik, K. S. (2005). MicroRNA-21 is an antiapoptotic factor in human glioblastoma cells. Cancer Res. *65*, 6029–6033.

Cheng, Y., Ji, R., Yue, J., Yang, J., Liu, X., Chen, H., Dean, D. B., and Zhang, C. (2007). MicroRNAs are aberrantly expressed in hypertrophic heart: do they play a role in cardiac hypertrophy? Am. J. Pathol. *170*, 1831–1840.

Chi, L., Zhang, S., Lin, Y., Prunskaite-Hyyrylainen, R., Vuolteenaho, R., Itaranta, P., and Vainio, S. (2004). Sprouty proteins regulate ureteric branching by coordinating reciprocal epithelial Wnt11, mesenchymal Gdnf and stromal Fgf7 signalling during kidney development. Development *131*, 3345–3356.

Cooklin, M., Wallis, W. R., Sheridan, D. J., and Fry, C. H. (1998). Conduction velocity and gap junction resistance in hypertrophied, hypoxic guinea-pig left ventricular myocardium. Exp. Physiol. *83*, 763–770.

Darrow, B. J., Fast, V. G., Kleber, A. G., Beyer, E. C., and Saffitz, J. E. (1996). Functional and structural assessment of intercellular communication. Increased conduction velocity and enhanced connexin expression in dibutyryl cAMP-treated cultured cardiac myocytes. Circ. Res. *79*, 174–183.

de Boer, T. P., van Rijen, H. V., Van der Heyden, M. A., Kok, B., Opthof, T., Vos, M. A., Jongsma, H. J., de Bakker, J. M., and van Veen, T. A. (2007). Beta-, not alpha-adrenergic stimulation enhances conduction velocity in cultures of neonatal cardiomyocytes. Circ. J. *71*, 973–981.

Ebert, M. S., Neilson, J. R., and Sharp, P. A. (2007). MicroRNA sponges: competitive inhibitors of small RNAs in mammalian cells. Nat. Methods *4*, 721–726.

Edwin, F., and Patel, T. B. (2008). A novel role of Sprouty 2 in regulating cellular apoptosis. J. Biol. Chem. *283*, 3181–3190.

Edwin, F., Singh, R., Endersby, R., Baker, S. J., and Patel, T. B. (2006). The tumor suppressor PTEN is necessary for human Sprouty 2-mediated inhibition of cell proliferation. J. Biol. Chem. *281*, 4816–4822.

Emdad, L., Uzzaman, M., Takagishi, Y., Honjo, H., Uchida, T., Severs, N. J., Kodama, I., and Murata, Y. (2001). Gap junction remodeling in hypertrophied left ventricles of aortic-banded rats: prevention by angiotensin II type 1 receptor blockade. J. Mol. Cell Cardiol. *33*, 219–231.

Farh, K. K., Grimson, A., Jan, C., Lewis, B. P., Johnston, W. K., Lim, L. P., Burge, C. B., and Bartel, D. P. (2005). The widespread impact of mammalian microRNAs on mRNA repression and evolution. Science *310*, 1817–1821.

Fong, C. W. *et al*. (2006). Sprouty 2, an inhibitor of mitogen-activated protein kinase signaling, is down-regulated in hepatocellular carcinoma. Cancer Res. *66*, 2048–2058.

Graham, F. L., and Prevec, L. (1991). Methods in Molecular Biology, Clifton, NJ: Humana Press Inc.

Gross, I., Armant, O., Benosman, S., de Aguilar, J. L., Freund, J. N., Kedinger, M., Licht, J. D., Gaiddon, C., and Loeffler, J. P. (2007). Sprouty2 inhibits BDNF-induced signaling and modulates neuronal differentiation and survival. Cell Death Differ. *14*, 1802–1812.

Hacohen, N., Kramer, S., Sutherland, D., Hiromi, Y., and Krasnow, M. A. (1998). sprouty encodes a novel antagonist of FGF signaling that patterns apical branching of the *Drosophila* airways. Cell *92*, 253–263.

Huebert, R. C. *et al*. (2004). Identification and regulation of Sprouty1, a negative inhibitor of the ERK cascade, in the human heart. Physiol. Genomics *18*, 284–289.

Humphreys, D. T., Westman, B. J., Martin, D. I., and Preiss, T. (2005). MicroRNAs control translation initiation by inhibiting eukaryotic initiation factor 4E/cap and poly(A) tail function. Proc. Natl. Acad. Sci. USA *102*, 16961–16966.

Hutvagner, G., Simard, M. J., Mello, C. C., and Zamore, P. D. (2004). Sequence-specific inhibition of small RNA function. PLoS Biol. *2*, 24.

Impagnatiello, M. A., Weitzer, S., Gannon, G., Compagni, A., Cotten, M., and Christofori, G. (2001). Mammalian sprouty-1 and -2 are membrane-anchored phosphoprotein inhibitors of growth factor signaling in endothelial cells. J. Cell Biol. *152*, 1087–1098.

Ji, R., Cheng, Y., Yue, J., Yang, J., Liu, X., Chen, H., Dean, D. B., and Zhang, C. (2007). MicroRNA expression signature and antisense-mediated depletion reveal an essential role of MicroRNA in vascular neointimal lesion formation. Circ. Res. *100*, 1579–1588.

Johnatty, S. E., Dyck, J. R., Michael, L. H., Olson, E. N., and Abdellatif, M. (2000). Identification of genes regulated during mechanical load-induced cardiac hypertrophy. J. Mol. Cell Cardiol. *32*, 805–815.

Kostin, S., Dammer, S., Hein, S., Klovekorn, W. P., Bauer, E. P., and Schaper, J. (2004). Connexin 43 expression and distribution in compensated and decompensated cardiac hypertrophy in patients with aortic stenosis. Cardiovasc. Res. *62*, 426–436.

Krutzfeldt, J., Rajewsky, N., Braich, R., Rajeev, K. G., Tuschl, T., Manoharan, M., and Stoffel, M. (2005). Silencing of microRNAs in vivo with 'antagomirs'. Nature *438*, 685–689.

Kwabi-Addo, B., Wang, J., Erdem, H., Vaid, A., Castro, P., Ayala, G., and Ittmann, M. (2004). The expression of Sprouty1, an inhibitor of fibroblast growth factor signal transduction, is decreased in human prostate cancer. Cancer Res. *64*, 4728–4735.

Lagos-Quintana, M., Rauhut, R., Yalcin, A., Meyer, J., Lendeckel, W., and Tuschl, T. (2002). Identification of tissue-specific microRNAs from mouse. Curr. Biol. *12*, 735–739.

Lao, D. H., Chandramouli, S., Yusoff, P., Fong, C. W., Saw, T. Y., Tai, L. P., Yu, C. Y., Leong, H. F., and Guy, G. R. (2006). A Src homology 3-binding sequence on the C terminus of Sprouty2 is necessary for inhibition of the Ras/ERK pathway downstream of fibroblast growth factor receptor stimulation. J. Biol. Chem. *281*, 29993–30000.

Lee, C. C., Putnam, A. J., Miranti, C. K., Gustafson, M., Wang, L. M., Vande Woude, G. F., and Gao, C. F. (2004). Over-expression of sprouty 2 inhibits HGF/SF-mediated cell growth, invasion, migration, and cytokinesis. Oncogene *23*, 5193–5202.

Lee, R. C., Feinbaum, R. L., and Ambros, V. (1993). The *C. elegans* heterochronic gene lin-4 encodes small RNAs with antisense complementarity to lin-14. Cell *75*, 843–854.

Lee, S. H., Schloss, D. J., Jarvis, L., Krasnow, M. A., and Swain, J. L. (2001). Inhibition of angiogenesis by a mouse sprouty protein. J. Biol. Chem. *276*, 4128–4133.

Lim, L. P., Lau, N. C., Garrett-Engele, P., Grimson, A., Schelter, J. M., Castle, J., Bartel, D. P., Linsley, P. S., and Johnson, J. M. (2005). Microarray analysis shows that some microRNAs downregulate large numbers of target mRNAs. Nature *433*, 769–773.

Lo, T. L. *et al*. (2004). The ras/mitogen-activated protein kinase pathway inhibitor and likely tumor suppressor proteins, sprouty 1 and sprouty 2 are deregulated in breast cancer. Cancer Res. *64*, 6127–6136.

Loffler, D. *et al*. (2007). Interleukin-6 dependent survival of multiple myeloma cells involves the Stat3-mediated induction of microRNA-21 through a highly conserved enhancer. Blood *110*, 1330–1333.

Malhotra, A., Reich, D., Reich, D., Nakouzi, A., Sanghi, V., Geenen, D. L., and Buttrick, P. M. (1997). Experimental diabetes is associated with functional activation of protein kinase C epsilon and phosphorylation of troponin I in the heart, which are prevented by angiotensin II receptor blockade. Circ. Res. *81*, 1027–1033.

Meister, G., Landthaler, M., Dorsett, Y., and Tuschl, T. (2004). Sequence-specific inhibition of microRNA- and siRNA-induced RNA silencing. RNA *10*, 544–550.

Meng, F., Henson, R., Wehbe-Janek, H., Ghoshal, K., Jacob, S. T., and Patel, T. (2007). MicroRNA-21 regulates expression of the PTEN tumor suppressor gene in human hepatocellular cancer. Gastroenterology *133*, 647–658.

Orom, U. A., Kauppinen, S., and Lund, A. H. (2006). LNA-modified oligonucleotides mediate specific inhibition of microRNA function. Gene *372*, 137–141.

Reich, A., Sapir, A., and Shilo, B. (1999). Sprouty is a general inhibitor of receptor tyrosine kinase signaling. Development *126*, 4139–4147.

Salameh, A., Frenzel, C., Boldt, A., Rassler, B., Glawe, I., Schulte, J., Muhlberg, K., Zimmer, H. G., Pfeiffer, D., and Dhein, S. (2006). Subchronic alpha- and beta-adrenergic regulation of cardiac gap junction protein expression. FASEB J. *20*, 365–367.

Sayed, D., Hong, C., Chen, I. Y., Lypowy, J., and Abdellatif, M. (2007). MicroRNAs play an essential role in the development of cardiac hypertrophy. Circ. Res. *100*, 416–424.

Schetter, A. J. *et al*. (2008). MicroRNA expression profiles associated with prognosis and therapeutic outcome in colon adenocarcinoma. Jama *299*, 425–436.

Si, M. L., Zhu, S., Wu, H., Lu, Z., Wu, F., and Mo, Y. Y. (2007). miR-21-mediated tumor growth. Oncogene *26*, 2799–2803.

Slaby, O., Svoboda, M., Fabian, P., Smerdova, T., Knoflickova, D., Bednarikova, M., Nenutil, R., and Vyzula, R. (2008). Altered expression of miR-21, miR-31, miR-143 and miR-145 is related to clinicopathologic features of colorectal cancer. Oncology *72*, 397–402.

Smith, J. H., Green, C. R., Peters, N. S., Rothery, S., and Severs, N. J. (1991). Altered patterns of gap junction distribution in ischemic heart disease. An immunohistochemical study of human myocardium using laser scanning confocal microscopy. Am. J. Pathol. *139*, 801–821.

Sood, A. K., Bhatty, R., Kamat, A. A., Landen, C. N., Han, L., Thaker, P. H., Li, Y., Gershenson, D. M., Lutgendorf, S., and Cole, S. W. (2006). Stress hormone-mediated invasion of ovarian cancer cells. Clin. Cancer Res. *12*, 369–375.

Spach, M. S., Heidlage, J. F., Dolber, P. C., and Barr, R. C. (2000). Electrophysiological effects of remodeling cardiac gap junctions and cell size: experimental and model studies of normal cardiac growth. Circ. Res. *86*, 302–311.

Sutterluty, H., Mayer, C. E., Setinek, U., Attems, J., Ovtcharov, S., Mikula, M., Mikulits, W., Micksche, M., and Berger, W. (2007). Down-regulation of Sprouty2 in non-small cell lung cancer contributes to tumor malignancy via extracellular signal-regulated kinase pathway-dependent and -independent mechanisms. Mol. Cancer Res. *5*, 509–520.

Tatsuguchi, M., Seok, H. Y., Callis, T. E., Thomson, J. M., Chen, J. F., Newman, M., Rojas, M., Hammond, S. M., and Wang, D. Z. (2007). Expression of microRNAs is dynamically regulated during cardiomyocyte hypertrophy. J. Mol. Cell Cardiol. *42*, 1137–1141.

Tefft, J. D., Lee, M., Smith, S., Leinwand, M., Zhao, J., Bringas, P., Jr., Crowe, D. L., and Warburton, D. (1999). Conserved function of mSpry-2, a murine homolog of *Drosophila* sprouty, which negatively modulates respiratory organogenesis. Curr. Biol. *9*, 219–222.

Uzzaman, M., Honjo, H., Takagishi, Y., Emdad, L., Magee, A. I., Severs, N. J., and Kodama, I. (2000). Remodeling of gap junctional coupling in hypertrophied right ventricles of rats with monocrotaline-induced pulmonary hypertension. Circ. Res. *86*, 871–878.

van Rooij, E., Sutherland, L. B., Liu, N., Williams, A. H., McAnally, J., Gerard, R. D., Richardson, J. A., and Olson, E. N. (2006). A signature pattern of stress-responsive microRNAs that can evoke cardiac hypertrophy and heart failure. Proc. Natl. Acad. Sci. USA *103*, 18255–18260.

Volinia, S. *et al*. (2006). A microRNA expression signature of human solid tumors defines cancer gene targets. Proc. Natl. Acad. Sci. USA *103*, 2257–2261.

Wu, L., Fan, J., and Belasco, J. G. (2006). MicroRNAs direct rapid deadenylation of mRNA. Proc. Natl. Acad. Sci. USA *103*, 4034–4039.

Yigzaw, Y., Cartin, L., Pierre, S., Scholich, K., and Patel, T. B. (2001). The C terminus of sprouty is important for modulation of cellular migration and proliferation. J. Biol. Chem. *276*, 22742–22747.

Yue, Y., Lypowy, J., Hedhli, N., and Abdellatif, M. (2004). Ras GTPase-activating protein binds to Akt and is required for its activation. J. Biol. Chem. *279*, 12883–12889.

Zhang, C., Chaturvedi, D., Jaggar, L., Magnuson, D., Lee, J. M., and Patel, T. B. (2005). Regulation of vascular smooth muscle cell proliferation and migration by human sprouty 2. Arterioscler Thromb. Vasc. Biol. *25*, 533–538.

Zhu, S., Si, M. L., Wu, H., and Mo, Y. Y. (2007). MicroRNA-21 targets the tumor suppressor gene tropomyosin 1 (TPM1). J. Biol. Chem. *282*, 14328–14336.

Zhuang, J., Yamada, K. A., Saffitz, J. E., and Kleber, A. G. (2000). Pulsatile stretch remodels cell-to-cell communication in cultured myocytes. Circ. Res. *87*, 316–322.